Bull. Mater. Sci., Vol. 37, No. 4, June 2014, pp. 903–909. © Indian Academy of Sciences.

Distinction between SnO_2 nanoparticles synthesized using co-precipitation and solvothermal methods for the photovoltaic efficiency of dye-sensitized solar cells

M M RASHAD[1], I A IBRAHIM[1], I OSAMA[1] and A E SHALAN[1,2,*]

[1]Central Metallurgical Research and Development Institute (CMRDI), P.O. Box 87, Helwan, Cairo, Egypt
[2]Institute of Materials for Electronics and Energy Technology (i-MEET),
Friedrich-Alexander-University of Erlangen-Nuremberg, Martensstraße 7, 91058 Erlangen, Germany

MS received 19 June 2013

Abstract. **Nanocrystalline SnO_2 powders prepared by solvothermal and co-precipitation pathways have been characterized using XRD, TEM, UV–Visible absorption, BET specific surface area (S_{BET}) method, EIS and *J–V* measurements. The obtained powders have a surface area and size of 38·59 m^2/g and 10·63 nm for the SnO_2 powders synthesized solvothermally at a temperature of 200 °C for 24 h, while the values were 32·59 m^2/g and 16·20 nm for the formed hydroxide precursor annealed at 1000 °C for 2 h by co-precipitation route. The microstructure of the formed powders appeared as tetragonal-like structure. Thus, the prepared SnO_2 nanopowders using two pathways were applied as an electrode in dye-sensitized solar cell (DSSC). The photoelectrochemical measurements indicated that the cell presents short-circuit photocurrent (J_{sc}), open circuit voltage (V_{oc}) and fill factor (FF) were 7·017 mA/cm^2, 0·690 V and 69·68%, respectively, for solvothermal route and they were 4·241 mA/cm^2, 0·756 V and 66·74%, respectively, for co-precipitation method. The energy conversion efficiency of the solvothermal SnO_2 powders was considerably higher than that formed by co-precipitation powders; ~3·20% (solvothermal) and 2·01% (co-precipitation) with the N719 dye under 100 mW/cm^2 of simulated sunlight, respectively. These results were in agreement with EIS study showing that the electrons were transferred rapidly to the surface of the solvothermal-modified SnO_2 nanoparticles, compared with that of a co-precipitation-modified SnO_2 nanoparticles.**

Keywords. **SnO_2 nanoparticle; co-precipitation method; solvothermal processes; dye-sensitized solar cells.**

1. Introduction

Dye-sensitized solar cells (DSSCs), which convert light to electricity by means of harvesting of solar radiation by the sensitizers, have been attracted considerable attention in scientific research and for practical applications (Shalan *et al* 2013b). The intrinsic advantages of these devices are high photoelectrical efficiency over a large span of the visible light spectrum under direct sunlight and diffuse light conditions. Moreover, it is low cost compared to the traditional solid-state crystalline silicon solar cells (Kuang *et al* 2007). Most of the dye-sensitized solar cells made from nanoporous SnO_2 photoelectrodes are sensitized with ruthenium (II) complexes (Thangadurai *et al* 2005). The investigation and development of the dye–semiconductor systems are essential for long-term applications of dye-sensitized solar cells. SnO_2 as a stable *n*-type semiconductor with a wide band gap (E_g = 3·6 eV) has been used for various applications, including solid-state gas sensor, photovoltaic devices, dye-based solar cells, transparent conductive films for display and solar cells, catalysis and anode materials of secondary lithium ion battery (Antonio *et al* 2003; Gu *et al* 2004; Kim and Shim 2006; Legendre *et al* 2007; Shalan *et al* 2013a). Although, SnO_2 is a good electron acceptor since its conduction band edge lies ~0·5 V more positive than that of TiO_2 (Stergiopoulos *et al* 2003), little significant works concerning dye-sensitized solar cells based on nanoporous SnO_2 photoanodes were published (Tian *et al* 2000). Recently, a number of methods have been used on the synthesis of nanosized SnO_2 such as sol–gel, spray pyrolysis, co-precipitation and solvothermal routes (Rashad *et al* 2009; Rashad and Ibrahim 2012a, b). Besides these techniques, co-precipitation is an alternative cheap and simple method for preparation of nanostructure material. So that, it is expected to find a wide applications among the processes commonly used for the preparation of nanosized SnO_2 (Chang *et al* 2004). In particular, the solvothermal method is an alternative to promote the crystallization under mild temperatures. Solvothermal treatments can be used to control the grain size, particle morphology, crystalline phases and surface chemistry by regulating the reaction temperatures, pressure, solvent

*Author for correspondence (a.shalan133@gmail.com)

nature, additives and aging time. Nanosized particles prepared using the solvothermal method is expected to have a large surface area, small particle size and a great stability. From the best of our knowledge, among the oxides reported, there are rare reports published about SnO_2 nanoparticles applied for DSSC, which are prepared using the solvothermal and co-precipitation methods. Moreover, this study aims to prepare two types of SnO_2 films, using solvothermal and co-precipitation pathways, for DSSC. The novelty of the present work is predicting the enhanced photovoltaic efficiency of the assembly SnO_2 DSSCs compared to the published work elsewhere (Gao *et al* 2012). The synthesized samples were characterized by XRD, TEM, UV–Vis spectroscopy, BET, EIS and *J–V* measurements. The photovoltaic performance of the two types of SnO_2/dye (N719) solar cell was evaluated from the overall conversion efficiency, fill factor, open circuit voltage and short-circuit current.

2. Experimental

2.1 *Materials and methods*

2.1a *Materials*: Chemically-grade stannic chloride pentahydrate ($SnCl_4{\cdot}5H_2O$) purchased from Sigma, Aldrich was used as a source of Sn^{4+} ion. Sodium hydroxide (5 M), (Fluka) was used as a base to attain the desired pH value of 10 for both solvothermal and co-precipitation methods. Fluorinated tin oxide (FTO) (Asahi Glass Co. Ltd) and indium tin oxide (ITO) glass substrates bought from SOLEMS, 10 and 70 $\Omega\ cm^{-2}$, are cleaned with soap water, milli-Q water, acetone and ethanol (99·5%) for 10 min before use. The substrates were dried under an N_2 flux and finally cleaned for 20 min in an UV-surface decontamination system (Novascan, PSD-UV) connected to an O_2 gas source. Synthetic air (premier quality), O_2 (BIP quality) and N_2 (BIP quality $< 0{\cdot}02\%$ O_2) purchased from Carburos Metalicos (Air Products) were used at $< 0{\cdot}5$ bar pressure. The dye solution is prepared by dissolving 0·17 mM cis-di-(thiocyanato)bis(2,2′-bipyridyl-4,4′-dicarboxylate) ruthenium-(II) (also called N719, Solaronix SA, Switzerland) in dry ethanol (from Sigma, Aldrich). An electrolyte made with 0·1 M lithium iodide (LiI) (Aldrich), 0·1 M iodine (I_2) (Aldrich), 0·6 M tetrabutylammonium iodide (Fluka) and 0·5 M tert-butylpyridine (Aldrich) in dry acetonitrile (Fluka).

2.1b *Methods (preparation of SnO_2 nanoparticles)*: Two types of SnO_2 particles were prepared using common co-precipitation and solvothermal-modified methods. In a typical procedure for solvothermal route, SnO_2 nanostructured was prepared by dissolving ($SnCL_4{\cdot}5H_2O$) in methanol, then NaOH solution dissolving in methanol was added gradually with stirring to adjust pH at 10. The resulting white solution was poured into the stainless steel autoclave for solvothermal method. The autoclave was sealed and maintained at 200 °C for 24 h, then cooled to room temperature naturally. A white precipitate was collected and washed with deionized water and methanol several times to remove impurities. The final product was dried at 80 °C overnight forming SnO_2 nanopowders. The same happened for co-preciptation route by dissolving tin chloride pentahydrate ($SnCl_4{\cdot}5H_2O$) with an aqueous sodium hydroxide (NaOH) solution (5 M) and adjust pH at desired values 10. The resulting milky white precipitate in each case was collected, filtered, washed with distilled water for several times to remove impurities, and then dried at 80 °C for 24 h. The prepared SnO_2 nanopowders were annealed at 1000 °C for 2 h.

2.2 *Preparation of photoanodes*

1 g portion of SnO_2 nanopowders (prepared by co-precipitation or solvothermal methods) were added to 1 mL of distillated water, 5 mL of absolute ethanol and stirred by magnetic stirrer for 10 h. Fluorinated tin oxide (FTO) glass substrates were cleaned with soap water, milli-Q water, acetone and ethanol (99·5%) for 10 min before use. The substrates were dried under an N_2 flux and finally cleaned for 20 min in a UV-surface decontamination system (Novascan, PSD-UV) connected to an O_2 gas source. Deposit a TiO_2 blocking layer by using titanium tetra chloride ($TiCl_4$). The reason for processing $TiCl_4$ at each electrode, the initial $TiCl_4$ treatment influences positively the SnO_2 working electrode in two manners, first, through enhancing the bonding strength between the FTO substrate and the SnO_2 layer and second, by blocking the charge recombination between electrons emanating from the FTO and the I_3^- ions present in the I^-/I_3^- redox couple. Then, the edges of clean FTO glass (15 Ω/sq) covered with adhesive tapes as the frame. Paste was flattened with a glass rod. Film thickness could be controlled by changing the concentration of the paste and the layer numbers of the adhesive tape (Scotch, 50 μm). Then, the films were dried under ambient conditions and then, annealed at 450 °C for 30 min to remove the binders in the paste and increase the crystallinity of the nanopowders. After calcination, the films were cooled down to 80 °C for dye sensitization. Dye sensitization was achieved by immersing the SnO_2 nanoparticle electrodes scattering layer in a 0·3 mM N719 dye (Solaronix) in ethanol solution overnight, followed by rinsing in ethanol and drying in air.

2.3 *Fabrication of DSSCs*

The sensitized SnO_2 film was rinsed with ethanol solution and assembled with a platinum-covered FTO electrode (15 Ω/sq) containing a hole in a sandwich-type configuration using sealing technique. The counter electrode was

prepared by adding 50 nm layer of platinum (Pt) on the surface, using spin coating pyrolysis technique. The two electrodes were sealed with a 25 μm thick polymer spacer (Surlyn, DuPont). The void between the electrodes was then filled with an iodide/tri-iodide based electrolyte, containing 0·5 M lithium iodide, 0·05 M iodine and 0·1 M 4-tert-butylpyridine in 1 : 1 acetonitrile propylene carbonate and sandwiched between the photoanode and the platinized counter electrode by firm press, via air pump vacuum backfilling through a hole pierced through the Surlyn sheet. The hole then was sealed with an adhesive sheet and a thin glass to avoid leakage of the electrolyte. The resulting cell had an active area of about 0·25 cm^2.

2.4 *Physical characterization*

Crystallite phases present in the different annealed samples were identified by X-ray diffraction (XRD) on a Brucker axis D8 diffractometer with crystallographic data software Topas 2 using CuKα (λ = 1·5406) radiation operating at 40 kV and 30 mA at a rate of 2°/min. The diffraction data were recorded for 2θ values between 20 and 80°. Transmission electron microscopy (TEM) was performed with a JEOL-JEM-1230 microscope. Nitrogen adsorption–desorption isotherms were obtained on an ASAP 2020 (Micromeritics Instruments, USA) nitrogen adsorption apparatus. All the samples degassed at 180 °C prior to Brunauer–Emmett–Teller (BET) measurements. BET specific surface area (S_{BET}) was determined by a multipoint BET method using the adsorption data in the relative pressure, P/P_0 in the range of 0·05–0·25. The desorption isotherm was used to determine the pore-size distribution using the Barret–Joyner–Halender (BJH) method. The nitrogen adsorption volume at P/P_0 = 0·995 was used to determine the pore volume and average pore size. The UV–Vis absorption spectrum was measured by a UV–VIS–NIR scanning spectrophotometer (Jasco-V-570 Spectrophotometer, Japan). Photocurrent–voltage *J–V* characteristic curves measurements were performed using the solar simulation, which was carried out with a Steuernagel Solarkonstant KHS1200. Light intensity adjusted at 1000 W/m^2 with a bolometric Zipp & Konen CM-4 pyranometer. Calibration of the sun simulator made by several means, with a calibrated S1227-1010BQ photodiode from Hamamatsu and a mini spectrophotometer from Ava-Spec 4200. The 1 Sun AM 1·5 simulated sunlight reference spectrum according to an ASTM G173 standard. Solar decay and IV-curves measured using a Keithley 2601 multimeter connected to a computer and software.

The photoelectric conversion efficiency (η) was calculated according to (1):

$$\eta\% = \frac{J_{SC} \cdot V_{OC} \cdot \mathrm{FF}}{P_{in}} \cdot 100. \quad (1)$$

The fill factor (FF) is the ratio between the maximum output power density available ($J_m \cdot V_m$) and the maximum power combining short-circuit and open-circuit situations (2) and it describes the 'squareness' of the *J–V* curve

$$\mathrm{FF}(\%) = \frac{J_m \cdot V_m}{J_{SC} \cdot V_{OC}} \cdot 100. \quad (2)$$

Impedance measurements (EIS) were performed with a computer-controlled potentiostat (EG & G, M273) equipped with a frequency response analyser (EG & G, M1025). The frequency range is 0·005–100 kHz. The magnitude of the alternative signal is 10 mV. Unless otherwise mentioned, all impedance measurements were carried out under a bias illumination of 100 mW/cm^2 (global AM 1·5, 1 sun) from a 450-W xenon light source. The obtained spectra were fitted with Z-View software (v2.1b, Scribner Associate Inc) in terms of appropriate equivalent circuits.

3. Results and discussion

3.1 *Crystal structure*

The sharp and high intensity peaks in X-ray diffraction (XRD) pattern, presented in figure 1, show that the two types SnO_2 nanostructures presented very good crystallization. All the reflection peak positions can be indexed as the cassiterite-characteristic modification of tetragonal SnO_2 phase. The diffraction peaks from the SnO_2 at 2θ = 26·5, 33·8, 37·8, 51·7, 54·6, 61·8, 64.7 and 66° related to the (110), (101), (200), (211), (220), (310), (112) and (301) diffraction planes were ascribed (Antonio *et al* 2003). The peak intensity of the solvothermal SnO_2 sample was slightly smaller and broader than that of the co-precipitation SnO_2 sample. The average crystallite size of the as-prepared SnO_2 was calculated from the most intense peak (110) plane of SnO_2 based on Debye Scherrer equation. The calculated crystallite sizes were 10·6 and 16·2 nm for the solvothermal and co-precipitation SnO_2 samples, respectively. Figure 1 shows TEM images of the particle shapes of two types of SnO_2 samples prepared by both co-precipitation and solvothermal methods. A relatively uniform mixture of tetragonal like structure particles with sizes ranging from 10 to 20 nm was observed in both samples. It could be observed that the nanocrystallite showed extra agglomerated status with mesoporous structures. The particles of the solvothermal-modified SnO_2 were slightly fine and smaller than those of the co-precipitation modified SnO_2 sample.

3.2 *Brunauer–Emmett–Teller (BET) measurements*

Analysing the hysteresis loop shapes of nitrogen isotherms gives information about pore structure in SnO_2

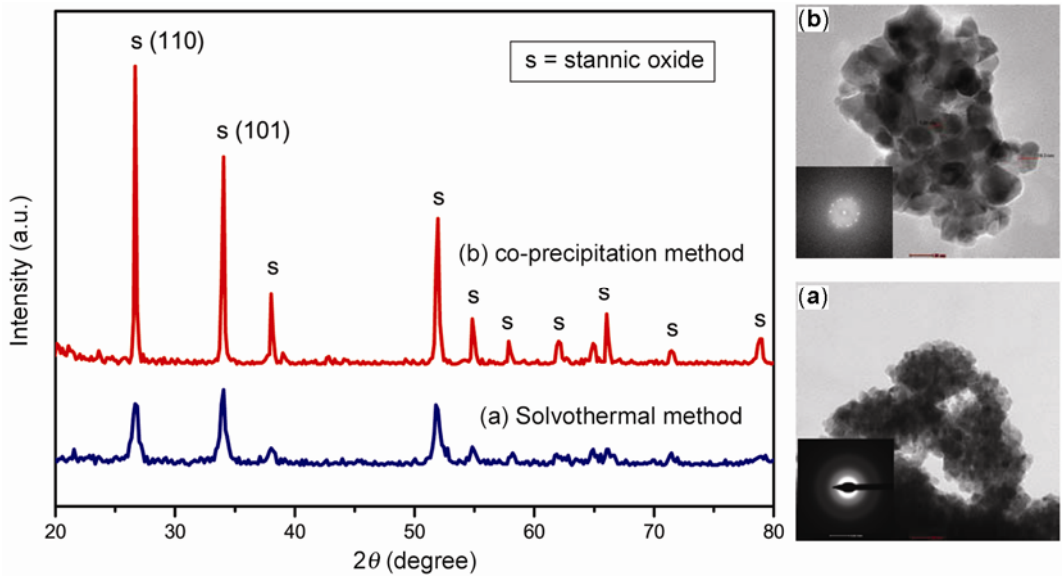

Figure 1. XRD patterns and TEM of the as-prepared samples using two methods (**a**) solvothermal method and (**b**) co-precipitation method, respectively.

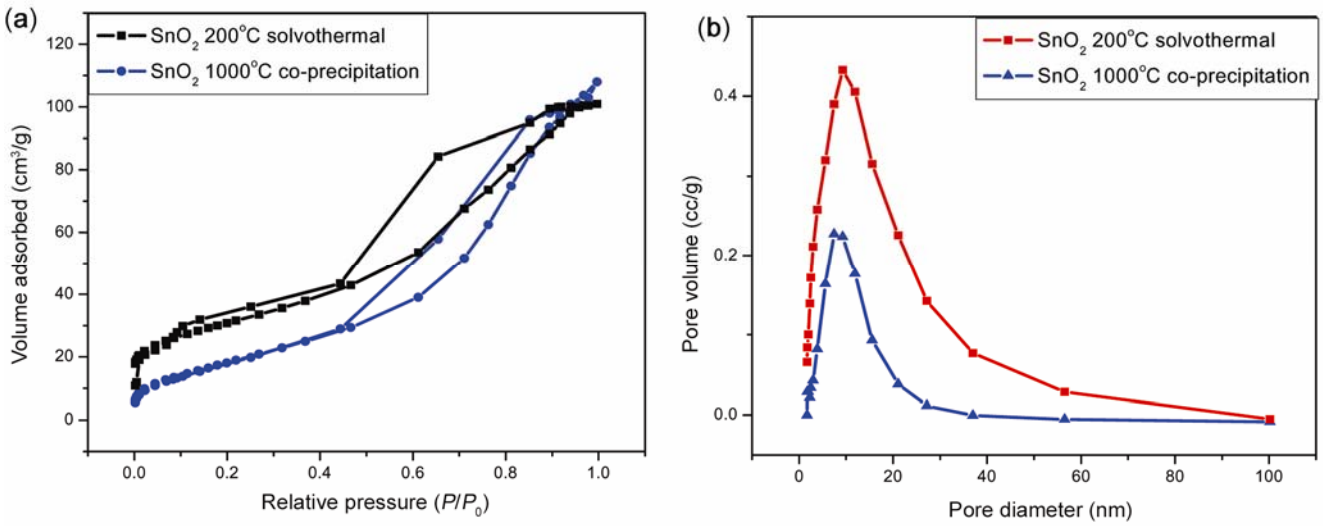

Figure 2. (**a**) N_2 adsorption–desorption isotherms surface area and (**b**) corresponding pore size distribution of the as-prepared samples using two methods: co-precipitation and solvothermal methods.

sample prepared by the two methods as shown in figure 2. All the samples show the type IV isotherms with type H_2 hysteresis loops according to Brunauer–Deming–Deming–Teller (BDDT) classification (Ba *et al* 2005; Rashad and El-Shall 2008), indicating the presence of mesoporous structure. The surface area, S_{BET} and the average pore radius were calculated as method reported elsewhere (Chang *et al* 2004). The surface area was 38·59 $m^2\ g^{-1}$ for 200 °C for 24 h via solvothermal process which is better than those of tin oxide powder synthesized via co-precipitation process that was 32·59 $m^2\ g^{-1}$ for 1000 °C for 2 h. The relatively high surface area of solvothermal SnO_2 compared to co-precipitation, one can be attributed to the extremely fine particle size. Moreover, the hysteresis loop would suggest that the shape of pore is a wide-mouth pore shape. The porous photoelectrode surface permits a better wetting of the powders by the electrolyte and finally results in a perfect penetration of the iodide/triiodide redox couple into the nanopowders pores, which in turn favour the interaction between the oxidized dye and regeneration of the sensitizer's ground state. Thus, the obtained results show that the electro-prepared SnO_2 nanoparticles demonstrate a great potential for use as electrode material in dye-sensitized solar

Table 1. Physical properties of SnO_2 nanoparticles prepared by co-precipitation and solvothermal methods.

Sample	S_{BET} ($m^2\ g^{-1}$)	Crystallite size (nm)	Pore volume ($cm^3\ g^{-1}$)	Average pore size (nm)	Porosity (%)	BJH adsorption (nm)	BJH desorption (nm)
SnO_2 co-precipitation 1000 °C	32·59	16·20	0·16	5·11	40	5·55	4·02
SnO_2 solvothermal 200 °C	38·59	10·63	0·16	4·26	42	6·58	4·95

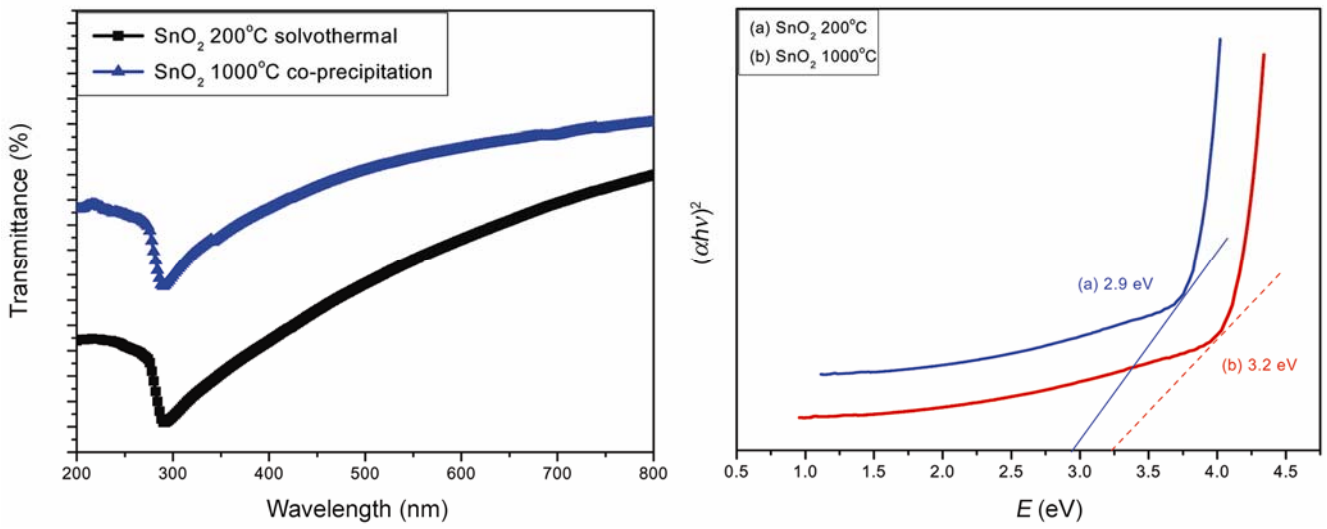

Figure 3. UV–Vis *T*% and band gap of the as-prepared samples using two methods (**a**) co-precipitation method and (**b**) solvothermal method, respectively.

cell. Table 1 list the physical properties of SnO_2 nanoparticles via two methods which can be evaluated from the S_{BET} measurements, as it found the difference in specific surface areas, porosity and relative rutile crystallinity in both the materials.

3.3 *UV–Vis spectroscopy and band gap energy*

The UV–Vis spectra of the two types of SnO_2 samples were obtained to determine the relationship between the solar energy conversion efficiency and spectroscopic properties, as shown in figure 3. The absorption band for the tetrahedral symmetry of Sn^{2+}, normally appears at ~295 nm. In the spectra of the solvothermal SnO_2 sample, the absorption bands were stronger and slightly red-shifted compared to those of the co-precipitation SnO_2 sample. Analysis of optical absorption spectra is one of the most productive tools for determining optical band gap of the obtained powders. From these spectral data, the absorption coefficient, α, was calculated using the relationship (El-Etre and Reda 2010; Rashad and Shalan 2012):

$$\alpha h\nu = A(h\nu - E_g)^m, \tag{3}$$

where α is the absorption coefficient that was calculated from the transmittance data, A an energy-independent constant, m a constant which determines type of the optical transition ($m = 3$ for direct forbidden transition, $m = 2$ for direct allowed transition) and E_g the optical band gap. The band gap in a semiconductor material is closely related to the wavelength range absorbed, where the band gap decreases with increasing absorption wavelength. It is believed that the solvothermal modification reduced the band gap of the SnO_2 semiconductor ($E_g = 2{\cdot}9$ eV) significantly compared to co-precipitation method ($E_g = 3{\cdot}2$ eV) and the bulk SnO_2 ($E_g = 3{\cdot}6$ eV) and due to the particle size of the prepared samples, as the particle size decreases, the band gap also decreases (Lee and Kang 2010). Furthermore, the formed powders show good results in photoactivity and dye solar cells.

3.4 *Photovoltaic performance*

Photocurrent–voltage characteristics of such a typical SnO_2 dye-sensitized solar cells samples synthesized using conventional solvothermal and co-precipitation methods under direct sunlight irradiation was measured and shown in figure 4. The fill factor, open-circuit voltage (V_{oc}), short-circuit current (J_{sc}), and overall energy efficiency were determined. A dye-sensitized solar cell assembled with co-precipitation-modified SnO_2 had an open-circuit voltage and short-circuit current density of 0·756 V and

Table 2. Comparison of *I–V* characteristics of DSSCs made from SnO_2 nanoparticles prepared by co-precipitation and solvothermal methods.

Sample	V_{oc}	J_{sc} (mA/cm^2)	FF	η (%)	Active area (cm^2)
SnO_2 co-precipitation 1000 °C	0·690	7·017	69·68	3·20	0·21
SnO_2 solvothermal 200 °C	0·756	4·241	66·74	2·01	0·18

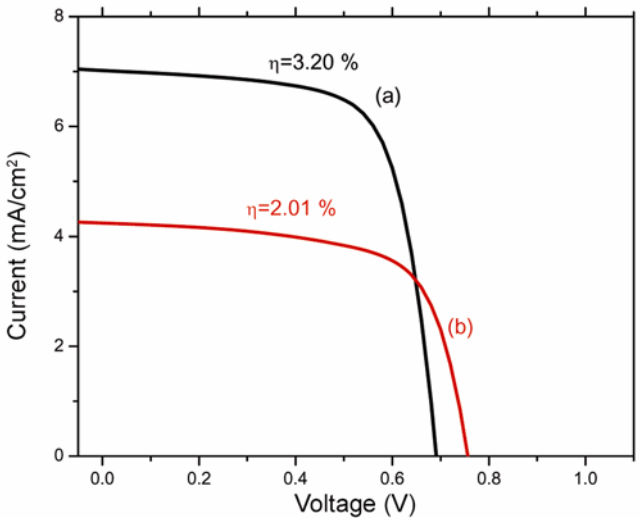

Figure 4. Comparison of the *I–V* characteristics of DSSCs made from (**a**) SnO_2 nanopowders solvothermal method and (**b**) SnO_2 nanopowders co-precipitation method.

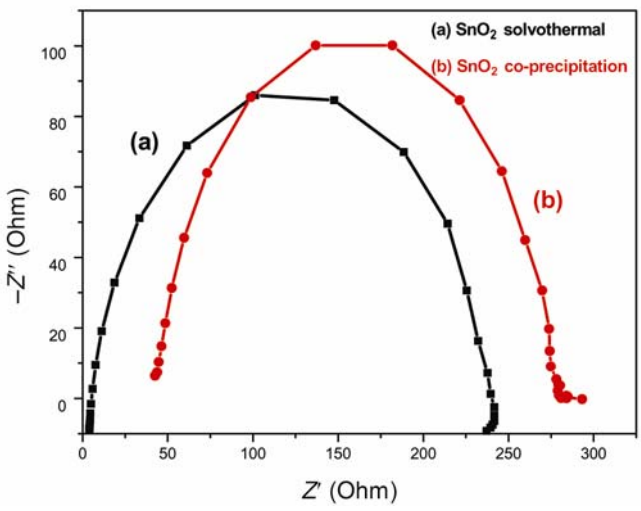

Figure 5. Nyquist diagrams of the impedance spectra of (**a**) DSSCs based on SnO_2 nanopowders solvothermal method compared to (**b**) DSSCs based on SnO_2 nanopowders co-precipitation method.

4·241 mA/cm^2, respectively, at an incident light intensity of 100 mW/cm^2. The power conversion efficiency of the co-precipitation-modified SnO_2 rutile structure was 2·01%. However, it was reached 3·20% in the DSSC made from the solvothermal-modified SnO_2 film; with an open-circuit voltage and short-circuit current density of 0·690 V and 7·017 mA/cm^2, respectively, as shown in table 2. From this result, it was confirmed that solvothermal-modified SnO_2 is a better material in DSSC than co-precipitation-modified SnO_2 (Lee *et al* 2010).

3.5 *Electrochemical impedance spectroscopy (EIS)*

Figure 5 shows typical electrochemical impedance spectra (EIS) of the DSSCs based on SnO_2 samples synthesized using solvothermal and co-precipitation methods. The Nyquist plots consist of two arcs. The first arc (not shown in figure) is in the high frequency region of 10^3–10^5 is attributed to the impedance related to the charge transfer process occurring at the counter electrode/electrolyte interface; while the second arc in the low frequency region of 1–10^3 Hz is attributed to the charge transfer at the SnO_2/electrolyte interface (Papageorgiou *et al* 1997). The present study employs EIS as a diagnostic tool for analysing in particular photovoltaic performance changes detected on dye-sensitized solar cells. An experimental model is presented interpreting the frequency response in terms of fundamental electronic and ionic processes occurring in the photovoltaic device. The wide frequency range of the EIS enables to measure wide scale internal resistances of each electrochemical step at the same time. DSSC is a complex system composed of several interfaces. A high electron accumulation must have occurred, because photogenerated electrons are not extracted at the electrode contact under illumination (Shalan *et al* 2013a, b). EIS data in this work are helpful for understanding of all the fabricated solar cells, and also can explain well, the existing interfaces in DSSCs. DSSCs based on SnO_2 prepared by solvothermal method possess the faster electron transfer rate and higher surface areas compared with DSSCs based on SnO_2 prepared by co-precipitation method. So, they had the highest η. The η value of DSSCs based on SnO_2 prepared by co-precipitation method decreased when compared to that of DSSCs based on SnO_2 prepared by solvothermal method. These results are in accordance with photoelectrical conversion efficiency data.

4. Conclusions

Dye-sensitized solar cells based on SnO_2 sample electrodes prepared by co-precipitation and solvothermal methods have been fabricated. The powders synthesized

by both routes were characterized by XRD, TEM, BET, UV–Vis spectroscopy, EIS and *I–V* characterization measurements. XRD shows that the formed SnO_2 has a tetragonal rutile crystal structure and the particle sizes observed in the transmission electron microscopy images were smaller in the solvothermal SnO_2 compared with the co-precipitation SnO_2 method. The absorption band of the solvothermal SnO_2 sample was slightly stronger and more red-shifted than the co-precipitation SnO_2 sample. Furthermore, solvothermal reduced the band gap of the SnO_2 semiconductor significantly compared to co-precipitation method, which resulted in better photoactivity. The solvothermal SnO_2 DSSC sample showed better solar energy conversion efficiency than that of co-precipitation SnO_2 sample. In 100 mW/cm^2-simulated sunlight, the solvothermal SnO_2 DSSC showed the following: solar energy conversion efficiency (η) = 3·20%, V_{oc} = 0·690 V, J_{sc} = 7·017 mA/cm^2 and fill factor = 69·68, while they were (η) = 2·01%, V_{oc} = 0·756 V, J_{sc} = 4·241 mA/cm^2 and fill factor = 66·74 for the co-precipitation-modified SnO_2 DSSC sample. EIS showed that electrons are transferred more rapidly to the surface of the solvothermal-modified SnO_2 film than that of the co-precipitation-modified SnO_2 nanoparticles.

References

Antonio J A T, Baez R G, Sebastian P J and Vàzquez A 2003 *J. Solid State Chem.* **174** 241

Ba J, Polleux J, Antonietti M and Niederberger M 2005 *Adv. Mater.* **17** 2509

Chang S T, Leu I C and Hon M H 2004 *J. Cryst. Growth* **273** 195

El-Etre A Y and Reda S M 2010 *Appl. Surf. Sci.* **256** 6601

Gao C, Li X, Lu B, Chen L, Wang Y, Teng F, Wang J, Zhang Z, Pan X and Xie E 2012 *Nanoscale* **4** 3475

Gu F, Wang S F, Lü M K, Cheng X F, Liu S W, Zhou G J, Xu D and Yuan D R 2004 *J. Cryst. Growth* **262** 182

Kuang D, Klein C, Ito S, Moser J -E, Humphry-Baker R, Evans N, Duriaux F, Grätzel C, Zakeeruddin S M and Grätzel M 2007 *Adv. Mater.* **19** 1133

Legendre F, Poissonnet S and Bonnailie P 2007 *J. Alloys Compd*. **434** 400

Lee Y and Kang M 2010 *Mater. Chem. Phys.* **122** 284

Lee Y, Chae J and Kang M 2010 *J. Ind. Eng. Chem.* **16** 609

Papageorgiou N, Maier W F and Grätzel M 1997 *J. Electrochem. Soc.* **144** 876

Rashad M M, Elsayed E M, Moharam M M, Abou-Shahbab R M and Saba A E 2009 *J. Alloys Compd.* **486** 759

Rashad M M and Ibrahim I A 2012a *J. Mater. Sci. Mater. Electron.* **23** 882

Rashad M M and Ibrahim I A 2012b *Mater. Technol.* **27** 308

Rashad M M and El-Shall H 2008 *Powder Technol.* **183** 161

Rashad M M and Shalan A E 2012 *Int. J. Nanoparticles* **5** 159

Shalan A E, Rashad M M, Yu Y, Lira-Cantú M and Abdel-Mottaleb M S A 2013a *Appl. Phys.* **A110** 111

Shalan A E, Rashad M M, Yu Y, Lira-Cantu M and Abdel-Mottaleb M S A 2013b *Electrochim. Acta* **89** 469

Kim H W and Shim S H 2006 *J. Alloys Compd.* **426** 286

Stergiopoulos T, Arabatzis I M, Cachet H and Falaras P 2003 *J. Photochem. Photobiol. A: Chem.* **155** 163

Thangadurai P, Bose A C, Ramasamy S, Kesavamoorthy R and Ravindran T R 2005 *J. Phys. Chem. Solids* **66** 1621

Tian H, Liu P H, Zhu W, Gao E, Wu D J and Cai S 2000 *J. Mater. Chem.* **10** 2708